Characterization of thrombopoietin (TPO)-responsive progenitor cells in adult mouse bone marrow with in vivo megakaryocyte and erythroid potential

Ashley P. Ng[a,1,2], Maria Kauppi[a,1], Donald Metcalf[a,b,2], Ladina Di Rago[a], Craig D. Hyland[a], and Warren S. Alexander[a,b]

[a]The Walter and Eliza Hall Institute of Medical Research, Parkville, Victoria 3052, Australia; and [b]Department of Medical Biology, University of Melbourne, Parkville, Victoria 3010, Australia

Contributed by Donald Metcalf, December 29, 2011 (sent for review November 14, 2011)

Hematopoietic progenitor cells are the progeny of hematopoietic stem cells that coordinate the production of precise numbers of mature blood cells of diverse functional lineages. Identification of cell-surface antigen expression associated with hematopoietic lineage restriction has allowed prospective isolation of progenitor cells with defined hematopoietic potential. To clarify further the cellular origins of megakaryocyte commitment, we assessed the in vitro and in vivo megakaryocyte and platelet potential of defined progenitor populations in the adult mouse bone marrow. We show that megakaryocytes arise from CD150^{+} bipotential progenitors that display both platelet- and erythrocyte-producing potential in vivo and that can develop from the Flt3^{-} fraction of the pregranulocyte-macrophage population. We define a bipotential erythroid-megakaryocyte progenitor population, the CD150^{+}CD9^{lo}endoglin^{lo} fraction of Lin^{-}cKit^{+}IL7 receptor alpha^{-}FcγRII/III^{lo}Sca1^{-} cells, which contains the bulk of the megakaryocyte colony-forming capacity of the bone marrow, including bipotential megakaryocyte-erythroid colony-forming capacity, and can generate both erythrocytes and platelets efficiently in vivo. This fraction is distinct from the CD150^{+}CD9^{hi}endoglin^{lo} fraction, which contains bipotential precursors with characteristics of increased megakaryocytic maturation, and the CD150^{+}CD9^{lo}endoglin^{hi} fraction, which contains erythroid lineage-committed cells. Finally, we demonstrate that bipotential erythroid-megakaryocyte progenitor and CD150^{+}CD9^{hi}endoglin^{lo} cells are TPO-responsive and that the latter population specifically expands in the recovery from thrombocytopenia induced by anti-platelet serum.

Adult hematopoietic progenitor cells are derived from hematopoietic stem cells (HSCs) in the bone marrow and coordinately produce precise numbers of mature hematopoietic cells of diverse functional lineages. Unlike HSCs, which are rare, hematopoietic progenitors comprise a significant proportion of the adult bone marrow and can undergo significant expansion in times of hematopoietic stress, mediated in large part by hematopoietic cytokines (1). Semisolid agar culture was the first in vitro assay that allowed identification of the myeloid lineage potential of hematopoietic progenitor cells at a clonal level (2). Identification of cell-surface antigen expression associated with stem cell activity and lineage restriction allowed prospective isolation of progenitors with defined hematopoietic potential. In the mouse bone marrow, HSC activity is correlated with expression of cKit and Sca1 and the absence of expression of markers of mature hematopoietic cells of multiple lineages (3, 4). Progenitor cells, defined by in vitro colony-forming activity, are located mainly within the Lin^{-}Kit^{+}Sca1^{-} fraction (5). This population can be subdivided further using FcγRII/III and CD34 surface markers (6) to define a common myeloid progenitor (CMP) (CD34^{+}FcγRII/III^{-}) as well as populations enriched for restricted granulocyte-macrophage potential (GMP) (CD34^{+}FcγRII/III^{+}) and megakaryocyte and erythroid potential (MEP) (CD34^{-}FcγRII/III^{-}). The CMP population proved heterogeneous, with Flt-ligand receptor (Flk2/Flt3) and PU.1 expression allowing segregation into granulocyte-monocyte-restricted (Flt3$^{+/-}$PU.1^{hi}) or megakaryocyte/erythroid-restricted (Flt3^{-}PU.1^{lo}) progenitor populations (7).

Defining hematopoietic progenitor cells with megakaryocyte and erythroid potential has been complicated by the emergence of several immunophenotypic definitions for megakaryocyte and megakaryocyte/erythroid bipotential progenitors. CD41 (the integrin IIb subunit), CD150 (the founding member of the SLAM family of cell surface receptors), and CD9 (a member of the tetraspanin superfamily) have been used in various combinations to define progenitors with megakaryocyte lineage potential within the Lin^{-}cKit^{+} pool (Table S1) (8–10). However, none of these antigens appears to be unique to megakaryocyte-restricted cells. For instance, although CD41 expression has been used to define a population of megakaryocyte progenitors (9), ganciclovir treatment of cells expressing thymidine kinase driven by the CD41 promoter leads to suppression of early erythroid-megakaryocytic progenitors in vivo and in vitro (11).

To clarify further the cellular precursors of committed megakaryocyte cells, we undertook a functional assessment of megakaryocyte and platelet potential within the adult mouse bone marrow. We defined a CD150^{+}CD9^{lo}endoglin^{lo} fraction of the Lin^{-}cKit^{+}IL-7 receptor α–negative (IL7Rα^{-})FcγRII/III^{lo}Sca1^{-} progenitor population that contains bipotential erythroid-megakaryocyte progenitors (BEMPs). This fraction is distinct from (*i*) the CD150^{+}CD9^{hi}endoglin^{lo} fraction, which contains bipotential precursors with characteristics of increased megakaryocytic maturation and which expands in response to TPO stimulation and anti-platelet serum (APS)-induced thrombocytopenia and (*ii*) the CD150^{+}CD9^{lo}endoglin^{hi} fraction, which contains erythroid lineage-committed cells. We also demonstrate that megakaryocyte progenitor cells defined via expression of CD41 retain erythroid potential and that the Flt3^{-} fraction of the previously defined pregranulocyte-macrophage (PreGM) population contains progenitors capable of forming megakaryocytes and erythroid progenitors in addition to granulocyte/monocyte-forming cells (9).

Results

To determine the relative contribution of progenitors in mouse adult bone marrow to megakaryocyte production using semisolid culture assays, we initially fractionated the Lin^{-}cKit^{+}IL7Rα^{-}FcγRII/III^{lo}endoglin^{lo} population in mouse adult bone marrow using Sca1 as well as CD150 and CD48 (Fig. S1 and *SI Materials and Methods*). CD150 has been implicated as a marker of megakaryocyte potential within the hematopoietic progenitor cell pool (8, 9).

Author contributions: A.P.N., M.K., D.M., L.D.R., C.D.H., and W.S.A. designed research, performed research, analyzed data, and wrote the paper.

The authors declare no conflict of interest.

Freely available online through the PNAS open access option.

[1]A.P.N. and M.K. contributed equally to this work.

[2]To whom correspondence may be addressed. E-mail: ang@wehi.edu.au or metcalf@wehi.edu.au.

This article contains supporting information online at www.pnas.org/lookup/suppl/doi:10.1073/pnas.1121385109/-/DCSupplemental.

Consistent with previous studies (5), the Sca1$^+$ fraction of this population contained almost all the preprogenitor blast colony-forming capacity (CFC) as well as producing colonies containing a diverse range of myeloid cells, including ~1/10th of the megakaryocyte colony-forming potential of the starting population (Table 1, and Fig. S1). The majority of the megakaryocyte colony-forming potential was found within the Sca1$^-$ fraction. Megakaryocyte CFC potential was present within both the CD150$^+$Sca1$^-$ and CD150$^-$Sca1$^-$ fractions. The CD150$^+$Sca1$^-$ fraction contained approximately two-thirds of the megakaryocyte colony-forming potential of the initial population and generated megakaryocyte-containing colonies almost exclusively (Table 1 and Fig. S1). The CD150$^-$Sca1$^-$ fraction, which includes the previously defined PreGM progenitors (9), generated granulocyte-monocyte colonies as well as megakaryocyte-containing colonies (Table 1 and Table S1).

The identity of the megakaryocyte CFC within the CD150$^+$ progenitor cell population was investigated further by fractionating Lin$^-$cKit$^+$Sca1$^-$IL7Rα$^-$FcγRII/III^{lo}CD150$^+$ cells using CD9 and endoglin expression into three distinct subpopulations (Fig. 1*A*). Of these, the CD150$^+$CD9^{lo}endoglin^{hi} population corresponds to the previously defined pre colony forming unit-erythroid (PreCFU-E) population (Fig. 1*C* and Table S1) (9) and demonstrated erythroblast morphology (Fig. 1*B*, *Right*), and the CD150$^+$CD9^{hi}endoglin^{lo} cells are immunophenotypically equivalent to previously defined CD9^{hi}MkPs (Fig. 1*C* and Table S1) (10) and showed features of early megakaryocyte differentiation (Fig. 1*B*, *Center*). The CD150$^+$CD9^{lo}endoglin^{lo} fraction was a population with an immature morphology without features of erythroid or megakaryocyte differentiation (Fig. 1*B*, *Left*). This fraction contained all the previously defined PreMeg-E cells (9) (Fig. 1*C* and Table S1), which comprised 85% of the CD150$^+$CD9^{lo}endoglin^{lo} population, as well as cells expressing CD41 (Fig. S2). Each of these populations was tested for colony-forming potential in vitro. Almost all the megakaryocyte colony-forming potential was within the CD150$^+$CD9^{lo}endoglin^{lo} fraction (Table 2). A third of the CFCs in this population were definitively bipotential, in that they generated colonies containing both megakaryocyte and erythroid cells. In contrast, the CD150$^+$CD9^{hi} population had limited clonogenic potential, with pure megakaryocyte colonies comprising more than 90% of colonies, in keeping with the more differentiated morphology of these cells. The CD150$^+$endoglin^{hi} PreCFU-E population had virtually no megakaryocyte colony-forming potential (Table 2). None of these fractions contained significant numbers of granulocyte, macrophage, or eosinophil colony-forming cells (Table 2).

In Vivo Potential of Lin$^-$cKit$^+$IL7Rα$^-$FcγRII/III^{lo}Sca1$^-$CD150$^+$ Fractions. To define the in vivo potential of progenitors within the Lin$^-$cKit$^+$IL7Rα$^-$FcγRII/III^{lo}Sca1$^-$CD150$^+$ population, we examined the contribution to the peripheral blood of recipient mice injected with GFP-marked subfractions (12). The CD9^{hi}endoglin^{lo} population rapidly generated platelets in vivo, with contribution evident within 4 d of transplantation, peak levels at day 7, and a decline thereafter (Fig. 2*A*). The CD9^{lo}endoglin^{lo} fraction exhibited significant and more sustained platelet-forming capacity. Compared with the CD150$^+$CD9^{hi} population, platelet production by this fraction was delayed but had not declined at 12 d after transplantation. Each of these populations also displayed robust erythrocyte-forming potential in vivo (Fig. 2*A*) but did not generate lymphoid or granulocyte/monocyte cells over this period. On the basis of this activity and clonogenic colony assays, we consider the Lin$^-$cKit$^+$IL7Rα$^-$FcγRII/III^{lo}Sca1$^-$CD150$^+$CD9^{lo}endoglin^{lo} fraction to be a bipotential erythroid megakaryocyte precursor (BEMP) population. As expected, the endoglin^{hi}CD9^{lo} PreCFU-E population produced erythrocytes but not platelets (Fig. 2*A* and Fig. S3). Intriguingly, and consistent with the ability to generate megakaryocyte-containing colonies in vitro, the CD150$^-$ component of the Lin$^-$cKit$^+$IL7Rα$^-$FcγRII/III^{lo}Sca1$^-$ bone marrow fraction, previously identified as a PreGM fraction (9), demonstrated equivalent, if not superior, platelet-generating capacity compared with the CD150$^+$ fractions, in combination with potent erythroid potential (Fig. 2*A*). Consistent with these activities, upon transplantation, GFP-marked PreGM cells generated both GMP and erythroid progenitors within the recipient bone marrow over 4–7 d, whereas granulocyte-macrophage potential was not evident from BEMP cells in the same assay (Fig. 2*B*). Of note, the production of erythroid progenitors from the PreGM fraction was delayed relative to the BEMP cells. This activity was confined to Flt3$^-$ progenitor cells within the PreGM fraction: Flt3$^+$ PreGM cells yielded granulocyte-monocyte colonies and GMP but few, if any, cells with erythroid-megakaryocyte potential, whereas Flt3$^-$ PreGM cells generated granulocyte-monocyte colonies and erythroid-megakaryocyte–containing colonies in vitro and GMP, colony forming unit-erythroid (CFU-E), and CD150$^+$ progenitors in vivo (Fig. S4*F* and Table S2).

Comparative Analysis of Progenitors with Erythroid-Megakaryocyte Potential. Flow cytometric analyses were used to determine the relationship of previously defined progenitors with megakaryocyte potential to the BEMP, CD9^{hi}endoglin^{lo}, and CD9^{lo}endoglin^{hi} fractions of the Lin$^-$cKit$^+$IL7Rα$^-$FcγRII/III^{lo}Sca1$^-$CD150$^+$ bone marrow population. The CD41$^-$ MEP population (Table S1) (8) was contained entirely within the BEMP and CD9^{lo}endoglin^{hi} fractions (Fig. S2), whereas the CD41^{hi}MkP population (9) (Table S1) was distributed between the BEMP and CD9^{hi}endoglin^{lo} fractions (Fig. S2). When purified GFP-marked populations were assayed for in vivo potential, CD9^{hi}MKPs, CD41^{hi}MKPs, and CD41$^-$MEPs all exhibited robust erythrocyte production in addition to production of platelets (Fig. 2*A*). Lin$^-$cKit$^+$IL7Rα$^-$FcγRII/III$^-$CD34$^-$Sca1$^-$ MEPs also generated red blood cells efficiently in vivo but were comparatively poor at producing platelets (Fig. 2*A*). It is noteworthy that CD41 expression in these enrichment

Table 1. CFC of fractions of Lin$^-$cKit$^+$IL7Rα$^-$ FcγRII/III^{lo}endoglin^{lo} adult bone marrow

	Colonies per 100 cells plated							
Fraction	Blast	G	GM	M	Eo	Meg	% cKit$^+$ fraction	Meg contribution (%)
Sca1$^-$CD48$^+$CD150$^-$	2 ± 1	14 ± 5	9 ± 2	10 ± 1	0 ± 0	7 ± 1	36 ± 2	21
Sca1$^-$CD48$^+$CD150$^+$	0.2 ± 0.2	0.1 ± 0.1	0.0 ± 0.1	0.3 ± 0.2	0 ± 0	24 ± 1	37 ± 2	68
Sca1$^+$	18 ± 5	1 ± 1	3.5 ± 4	9 ± 4	0 ± 0	3 ± 2	19 ± 1	11

Mean colony counts ± SD per 100 cells from four replicate experiments using a combined stimulus of SCF (100 ng/mL), IL-3 (10 ng/mL), and EPO (4 IU/mL). Eo, eosinophil; G, granulocyte; GM, granulocyte-macrophage; M, macrophage; Meg, megakaryocyte colonies, including colonies of megakaryocytes and erythroid cells; Meg contribution, percentage contribution to megakaryocyte CFC of each fraction, calculated by adjusting contribution to percetage of cKit$^+$ fraction by relative ability of cells to form megakaryocyte colonies; % cKit$^+$ fraction, percentage contribution of each fraction to Lin$^-$cKit$^+$ IL7Rα$^-$FcγRII/III^{lo}endoglin^{lo} bone marrow with means ± SD from four mice (Fig. S1).

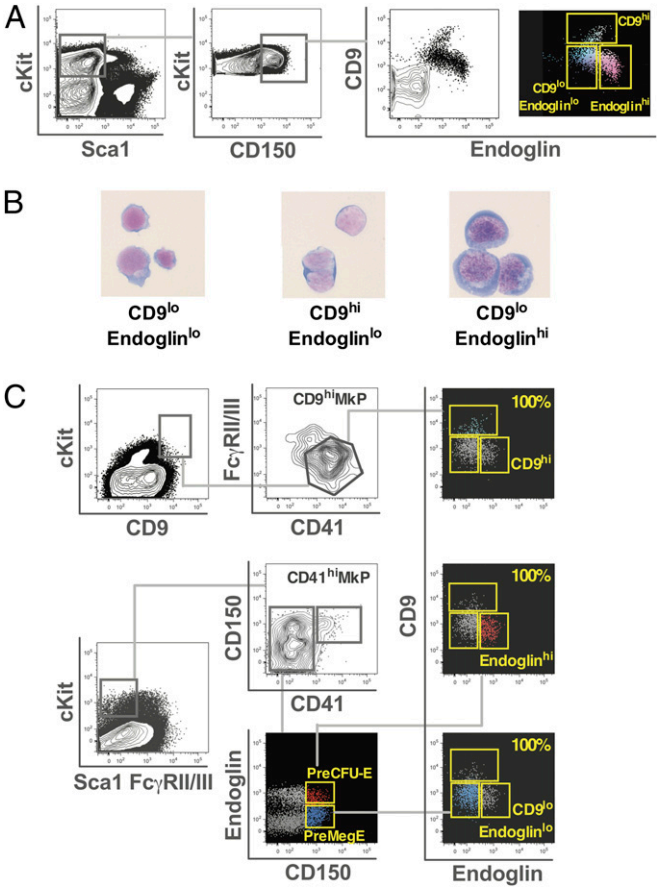

Fig. 1. Fractionation of Lin$^-$cKit$^+$Sca1$^-$IL7Rα$^-$FcγRII/III^{lo}CD150$^+$ bone marrow with CD9 and endoglin. (*A*) Flow cytometry fractionation of Lin$^-$cKit$^+$Sca1$^-$IL7Rα$^-$FcγRII/III^{lo}CD150$^+$ bone marrow cells by endoglin and CD9 expression into CD9^{lo}endoglin^{lo}, CD9^{hi}endoglin^{lo}, and CD9^{lo}endoglin^{hi} populations. Isotype control (contour plot). (*B*) CD9^{lo}endoglin^{lo} (*Left*), CD9^{hi}endoglin^{lo} (*Center*), and CD9^{lo}endoglin^{hi} (*Right*) cytocentrifuge preparations stained with May–Grunwald–Giemsa stain. (*C*) Comparison of CD9^{lo}endoglin^{lo}, CD9^{hi}endoglin^{lo}, and CD9^{lo}endoglin^{hi} Lin$^-$cKit$^+$Sca1$^-$IL7Rα$^-$FcγRII/III^{lo}CD150$^+$ bone marrow fractions with CD9^{hi}MkP, PreCFU-E, and PreMeg-E populations (Table S1) by flow cytometry.

schemes did not distinguish megakaryocyte-restricted progenitors from their bipotential counterparts. This finding is explained by the observation that CD41^{hi}MkPs overlap with CD150$^+$CD9^{lo}endoglin^{lo} BEMPs (Fig. S2). Like BEMPs, CD41$^-$ MEPs exhibited sustained production of both erythrocytes and platelets in vivo (Fig. 2*A*). In contrast, CD9^{hi} expression, exemplified in both CD9^{hi}MkPs and CD150$^+$CD9^{hi}endoglin^{lo} fractions, appeared to define a bipotential population with a unique pattern of transient platelet reconstitution (Fig. 2*A*), in keeping with cytomorphological features of more advanced megakaryocyte differentiation (Fig. 1*B*) and limited clonogenicity (Table 2).

Down-regulation of PU.1 expression is associated with restriction of myeloid progenitors to erythroid and megakaryocyte lineage fates (7). Consistent with their in vivo potential, PU.1 expression in bipotential BEMP and CD150$^+$CD9^{hi}endoglin^{lo} progenitors was significantly lower than observed in PreGM or GMP populations, and further down-regulation of PU.1 was evident in erythroid-restricted PreCFU-E and CFU-E bone marrow fractions (Fig. 2*C*).

BEMPs Are Responsive to TPO-Induced Megakaryocyte Differentiation in Vitro. In cultures containing a mixture of SCF, IL-3, and EPO (a general stimulus of myeloid, megakaryocytic, and erythroid cells), BEMPs generated both CD9^{hi}endoglin^{lo} and CD9^{lo}endoglin^{hi} cells during 4 d in culture, indicative of both megakaryocytes and erythroid cells as defined by morphological criteria (Fig. 3 *A* and *B* and *SI Materials and Methods*). Stimulation of BEMPs by TPO in combination with SCF resulted in an increase in the proportion of CD9^{hi}endoglin^{lo} cells and megakaryocytes produced, whereas the combination of EPO and SCF favored accumulation of CD9^{lo}endoglin^{hi} and recognizable erythroid cells (Fig. 3 *A* and *B*). TPO was a potent stimulus for megakaryocyte differentiation from BEMPs, with TPO+SCF-stimulated megakaryocytes displaying higher DNA ploidy than their EPO+SCF-stimulated counterparts (Fig. 3*C*). However, TPO was a relatively poor proliferative stimulus, even in combination with SCF, with the total number of cells generated from BEMPs significantly lower than that generated in response to EPO+SCF or SCF+IL-3+EPO (Fig. 3*D*). Consistent with the relatively low in vitro clonogenic potential and transient in vivo platelet-generating capacity of the CD150$^+$CD9^{hi}endoglin^{lo} fraction, these cells proliferated less than their BEMP counterparts but also were capable of responding to TPO and EPO with enhanced megakaryocytic and erythroid differentiation, respectively (Fig. 3*D* and Fig. S3). CD150$^+$CD9^{lo}endoglin^{hi} PreCFU-E cells readily generated erythroid cells in the presence of EPO but displayed negligible megakaryocyte differentiation in these assays (Fig. S3).

As expected from the analyses of in vivo potential, the PreGM population was capable of granulocyte/monocyte, erythroid, and megakaryocyte differentiation and expansion in vitro but, unlike BEMPs, did not show a proportional increase in megakaryocyte differentiation in response to TPO+SCF, presumably because of the significant granulocyte formation stimulated by SCF (Fig. S4 *A*–*E*).

CD150$^+$CD9^{hi}Endoglin^{lo} Cells Expand in Response to Excess TPO or APS-Induced Thrombocytopenia. We next examined the effect of supraphysiologic TPO signaling on the CD150$^+$ Lin$^-$cKit$^+$IL7Rα$^-$FcγRII/III^{lo}Sca1$^-$ population in vivo. Although the number of BEMPs was increased modestly in the bone marrow of *TPO*^{Tg} mice (13), CD150$^+$CD9^{hi}endoglin^{lo} early megakaryocyte differentiated bipotential progenitors proportionally doubled at the expense of CD150$^+$CD9^{lo}endoglin^{hi} PreCFU-E cells (Fig. 4*A*). Consistent

Table 2. CFP of fractions of Lin$^-$cKit$^+$Sca1$^-$IL7Rα$^-$FcγRII/III^{lo}CD150$^+$ adult bone marrow

	Clonogenic colonies per 100 cells plated							
Fraction	Blast	G	GM	M	Eo	Meg	% of CD150$^+$ fraction	Meg contribution (%)
CD9^{lo}endoglin^{lo} (BEMP)	0.5 ± 0.5	0.2 ± 2	0.2 ± 0.2	0.2 ± 0.2	0 ± 0	28 ± 9	51 ± 4.9	92
CD9^{hi}endoglin^{lo}	0.5 ± 0.6	0.1 ± 0.2	0.2 ± 0.4	0.3 ± 0.3	0 ± 0	10 ± 4	13 ± 2.3	8
CD9^{lo}endoglin^{hi} (PreCFU-E)	0 ± 0	0 ± 0	0.2 ± 0.3	0 ± 0	0 ± 0	0.5 ± 0.3	36 ± 5.8	0

Mean colony counts ± SD per 100 cells from four replicate experiments using a combined stimulus of SCF, IL-3, and EPO. Eo, eosinophil; G, granulocyte; GM, granulocyte-macrophage; M, macrophage; Meg, megakaryocyte colonies, including colonies of megakaryocytes and erythroid cells; Meg contribution, percentage contribution to megakaryocyte CFC of each fraction, calculated by adjusting contribution to percentage of CD150$^+$ fraction by relative ability of cells to form megakaryocyte colonies; % of CD150$^+$ fraction, percentage contribution each population to Lin$^-$cKit$^+$Sca1$^-$IL7Rα$^-$FcγRII/III^{lo}CD150$^+$ adult bone marrow with means ± SD from six mice.

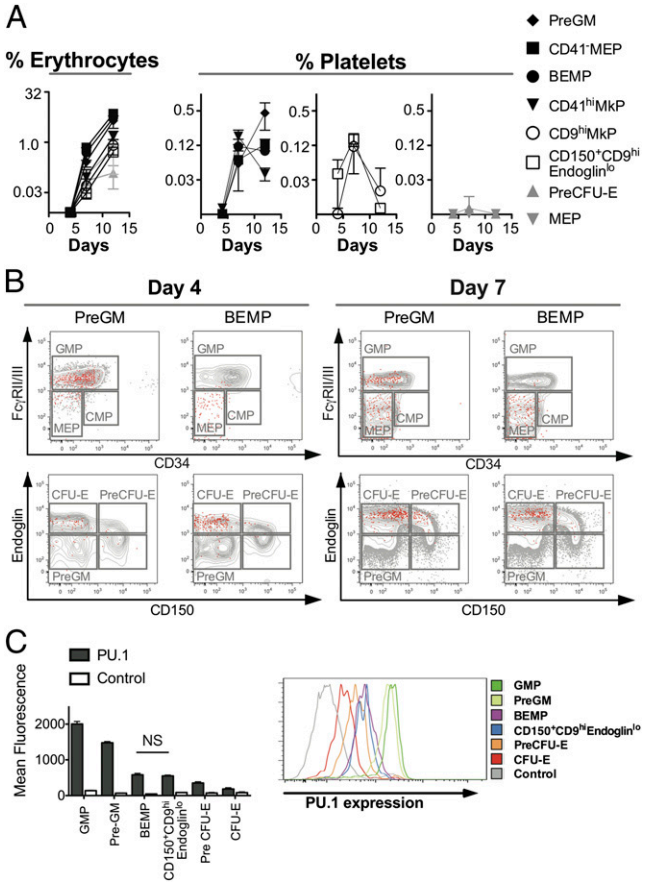

Fig. 2. In vivo potential of transplanted progenitor cells. One thousand GFP-marked cells (12) from purified cell populations were transplanted into sublethally irradiated recipients (*SI Materials and Methods*). (*A*) Percentage contribution to erythrocytes and platelets in peripheral blood from GFP-marked donor-derived cells on days 4, 7, and 12 after transplantation. Data shown are means ± SD from two or three independent donors each into three or four recipients. *y* axis is $\log_2$ scale. (*B*) Analysis of Lin$^-$cKit$^+$ bone marrow 4 and 7 d after transplantation with GFP-marked donor PreGM or BEMP cells. Formation of GMP, CMP, and MEP (*Upper*) and PreCFU-E, CFU-E (*Lower*) progenitor populations. Red, donor cells; gray, recipient cells. Representative analysis from three independent donors is shown. (*C*) Expression of *PU.1*^{gfp} (7) in arbitrary mean fluorescence intensity (MFI) units for each progenitor cell population indicated (Table 2 and Table S1). (*Left*) MFI means ± SD from four mice for each population. (*Right*) Representative MFI profiles. $P < 0.0001$ by repeated-measures ANOVA of all progenitor populations. Tukey's multiple comparison of means; $P < 0.05$ for comparison between all populations except between BEMPs and CD150$^+$CD9^{hi}endoglin^{lo} cells. NS, not significant.

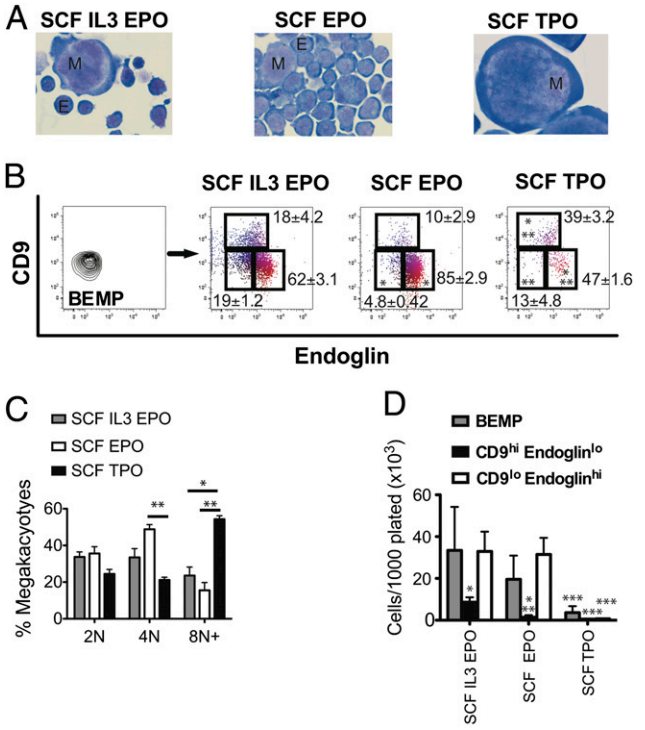

Fig. 3. In vitro responses of Lin$^-$cKit$^+$Sca1$^-$IL7Rα$^-$FcγRII/III^{lo}CD150$^+$ progenitor cells to cytokine stimulation. Liquid culture of sorted progenitor cells after 4 d with indicated cytokine combinations (SCF, 20 ng/mL; IL-3, 10 ng/mL; EPO, 2 IU/mL; TPO, 200 ng/mL). (*A*) Cytocentrifuge preparations stained with May–Grunwald–Giemsa of differentiated cells derived from BEMPs (magnification: 1,000×). E, erythroid; M, megakaryocyte. (*B*) Flow cytometry analysis. Blue, CD150$^+$CD9^{hi} megakaryocytes; red, CD150$^-$CD9^{lo}endoglin^{hi} erythroid progenitors. $*P_{adj} < 0.05$ compared with SCF, IL3, and EPO, $**P_{adj} < 0.05$ compared with SCF and EPO. (*C*) DNA ploidy of CD150$^+$CD9^{hi}endoglin^{lo} megakaryocytes generated from BEMPs. $*P_{adj} < 0.05$ compared with SCF, IL3, and EPO, $**P_{adj} < 0.05$ compared with SCF and EPO. (*D*) Proliferation of purified BEMP, CD9^{hi}endoglin^{lo}, and CD9^{lo}endoglin^{hi} cells. $*P_{adj} < 0.026$ comparing CD9^{hi}endoglin^{lo} with CD9^{lo}endoglin^{hi} progenitors. $**P_{adj} < 0.007$ comparing CD9^{hi}endoglin^{lo} with BEMP cells, $***P_{adj} < 0.007$ comparing SCF+TPO with SCF+IL3+EPO. Statistical analysis by unpaired *t* test of three biological replicates with Holm modification of Bonferroni correction for multiple testing.

with these effects reflecting increased TPO signaling, the converse was observed for each of these populations in *Mpl*$^{-/-}$ mice (14).

We then assessed whether perturbation of CD150$^+$ bipotential progenitor populations toward megakaryocyte differentiation could be induced by acute thrombocytopenia following treatment with APS. APS was administered to wild-type mice, and the numbers of CD150$^+$ bone marrow progenitors, bone marrow megakaryocytes, and peripheral blood platelets were analyzed during the subsequent days. As previously described, administration of APS resulted in rapid, severe thrombocytopenia, with platelet numbers falling to less than 5% of the pretreatment level within 2 h. Recovery was evident 2 d later, and platelet numbers returned to normal levels within 4 d of treatment (Fig. 4*B*). Expansion of the CD150$^+$CD9^{hi}endoglin^{lo} population was demonstrable on days 1, 2, and 4 after APS administration and thereafter returned to levels observed in control mice administered normal saline (Fig. 4*B*). The expansion of these progenitors coincided with the increase in bone marrow megakaryocyte number (Fig. 4*C*) and preceded the recovery in platelet count. The numbers of BEMPs and CD150$^+$CD9^{lo}endoglin^{hi} PreCFU-E cells did not alter significantly during the APS recovery period (Fig. 4*B*). The response to APS is likely to be driven to a significant extent by TPO, because rapid recovery of platelet numbers failed to occur in APS-treated *Mpl*$^{-/-}$ mice (Fig. 4*D*).

Discussion

Methods for identifying and isolating myeloid progenitor cell populations according to lineage potential using combinations of surface antigens are powerful tools in the understanding of physiologic and perturbed hematopoiesis. In this study, we investigated the phenotypic relationships and in vivo potential of progenitor cells with megakaryocyte potential; our findings are summarized in Fig. 5. Several cell-surface markers, including CD150, CD9, and CD41, have proven useful in defining megakaryocyte potential (Table S1). Here we show that two-thirds of the megakaryocyte colony-forming activity in the adult mouse bone marrow resides in the CD150$^+$ fraction of the Lin$^-$cKit$^+$IL7Rα$^-$FcγRII/III^{lo}Sca1$^-$ progenitor cell pool, primarily within a CD9^{lo}endoglin^{lo} pop-

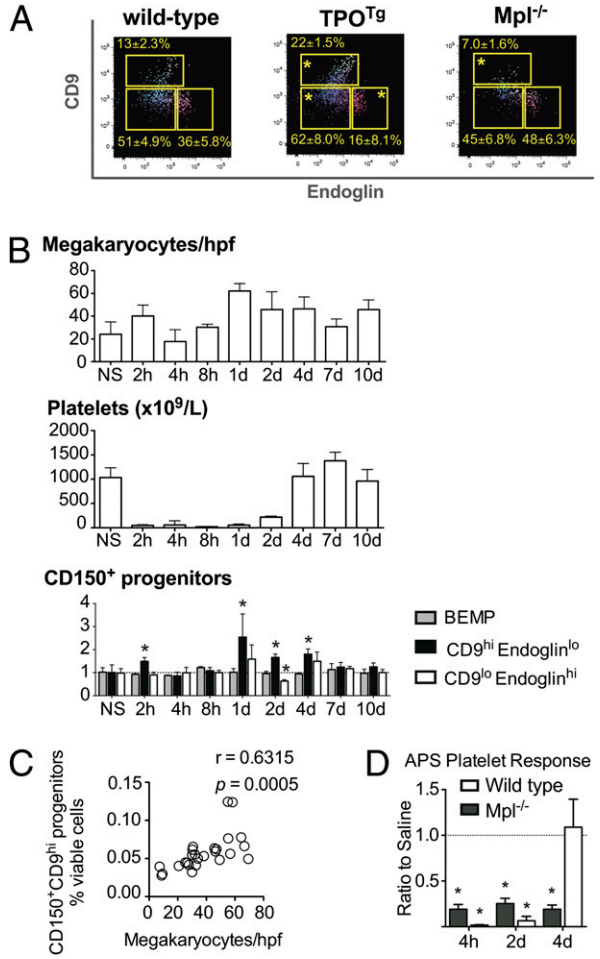

Fig. 4. Responses of Lin⁻cKit⁺Sca1⁻IL7Rα⁻FcγRII/III^{lo}CD150⁺ progenitor cells to excess TPO and APS treatment in vivo. (*A*) BEMP, CD9^{hi}endoglin^{lo}, and CD9^{lo}endoglin^{hi} populations in wild-type, *TPO*^{Tg} (13), and *Mpl*$^{-/-}$ (14) mice. Relative proportions are shown as means ± SD from six mice per genotype. *P_{adj} < 0.04 for comparison with wild-type by unpaired *t* test, with Holm modification of Bonferroni correction for multiple testing. (*B–D*) Analysis of mice treated with APS. (*B*) (*Top*) Megakaryocytes per high-powered field (hpf) across sternum and femur sections. (*Middle*) Peripheral blood platelet count. (*Bottom*) Ratio of BEMP, CD9^{hi}endoglin^{lo}, and CD9^{lo}endoglin^{hi} cells after APS treatment compared with normal saline-treated controls. Data shown are mean ± SD from six mice per time point. *P < 0.02 by unpaired *t* test, demonstrating an absolute increase in CD9^{hi}endoglin^{lo} cells at 2 h, day 1, day 2, and day 4 after APS and a decrease in CD9^{lo}endoglin^{hi} progenitors at day 2 after APS. (*C*) The number of CD150⁺CD9^{hi}endoglin^{lo} cells per viable bone marrow cell compared with the number of megakaryocytes per hpf following APS, with Pearson correlation coefficient (*r*) and *P* value shown. (*D*) Response of *Mpl*$^{-/-}$ and wild-type mice following APS. The relative number of platelets after APS treatment relative to normal saline-treated genotype-matched mice. Data shown are mean ± SD from three to six mice per genotype for each treatment. *P < 0.002 by Student's two-tailed *t* test.

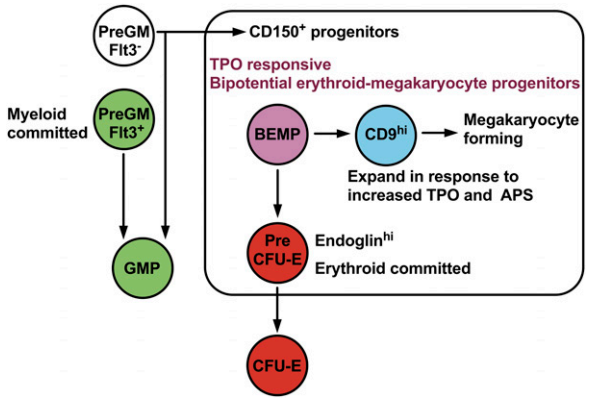

Fig. 5. Origin of erythroid and megakaryocyte progenitors. Lineage restriction, suggested hierarchical relationships, and response of myeloid progenitor cell populations examined to TPO or APS. Refer to Table S1 for details of immunophenotypes of PreGM (white, green), GMP (green), Pre-CFU-E (red), and CFU-E (red) and to Fig. 1*A* for definitions of CD9^{lo}endoglin^{lo} BEMP (light purple) and CD9^{hi}endoglin^{lo} (blue) progenitor populations.

ulation, from which definitive bipotential clones were identified by semisolid agar colony assays. In vivo assays confirmed megakaryocyte lineage potential within this population, which readily generated platelets in transplanted mice. Although this population was unable to produce lymphoid or granulocyte/monocyte cells, its potent erythroid potential also was evident in vivo, leading us to consider this population as containing BEMPs. Unlike prior definitions of bipotential progenitors (Table S1), a proportion of BEMPs express CD41. The CD9^{hi}endoglin^{lo} component of the CD150^{+} progenitor fraction retained bipotential platelet-erythroid potential in vivo but, unlike BEMPs, included cells with morphological characteristics of increased megakaryocyte differentiation. Indeed, in vivo, the CD9^{hi}endoglin^{lo} population generated platelets more quickly and more transiently than BEMPs. These observations, combined with the reduced megakaryocyte colony-forming activity of the CD9^{hi}endoglin^{lo} population relative to BEMPs, implies that the former population contains more mature, less proliferative megakaryocyte/platelet progenitors. The CD9^{lo}endoglin^{hi} portion of the CD150^{+} progenitor fraction has been described previously as a "PreCFU-E population" (9) and, as anticipated, lacked megakaryocyte CFC and in vivo platelet potential but produced red blood cells efficiently. These observations are consistent with a process of maturation in which the CD9^{lo}endoglin^{lo} BEMPs are the precursors of CD9^{hi}endoglin^{lo} and CD9^{lo}endoglin^{hi} daughter populations, the up-regulation of CD9 being a marker of retained megakaryocyte potential and acquisition of high endoglin expression correlating with erythroid restriction.

An unexpected outcome of the in vivo comparison of distinct bone marrow fractions with megakaryocyte progenitor activity was the observation that all such populations displayed significant erythroid lineage potential in addition to platelet-generating capacity. MkPs defined via expression of CD9 (CD9^{hi}MkP; Table S1) or CD41 (CD41^{hi} MkP; Table S1) both readily generated red blood cells when transplanted into recipient mice. Indeed, none of the populations examined displayed purely megakaryocyte/platelet restriction in vivo. The final stages of megakaryocyte differentiation therefore may involve production of immature megakaryocytes or precursors with low proliferative potential directly from bipotential progenitor cells.

It also is noteworthy that the PreGM population, defined as the CD150⁻endoglin⁻ fraction of the Lin⁻cKit⁺IL7Rα⁻FcγRII/III^{lo}Sca1⁻ progenitor cell pool, exhibited megakaryocyte CFC in vitro and the capacity to produce platelets and erythrocytes in vivo. Previous studies with this PreGM fraction identified modest production of megakaryocytes and erythroid cells in vitro and platelet potential in vivo (9). Our results showed not only that the PreGM population has in vivo erythroid potential but also that, on a per-cell basis, erythroid-megakaryocyte activity appeared as potent as that displayed by the restricted BEMP populations under study. This activity was restricted to Flt3⁻ PreGM cells. Because GMP, CFU-E, and CD150^{+} cells could develop from these cells in vivo, this result suggests that common myeloid progenitor cells may reside within this fraction.

Among the fractions of the Lin⁻cKit⁺IL7Rα⁻FcγRII/III^{lo}Sca1⁻ CD150^{+} compartment defined by levels of CD9 and endoglin ex-

pression, in vivo expansion of the $CD9^{hi}endoglin^{lo}$ population was most prominent in response to elevated TPO concentration in transgenic mice and was reduced selectively in mice lacking the TPO receptor, c-Mpl. Because the proliferative capacity of the $CD9^{hi}endoglin^{lo}$ fraction in cultures containing TPO was relatively low, it seems likely that the TPO-driven expansion of $CD9^{hi}endoglin^{lo}$ cells is driven in significant part by the maturation of precursors such as BEMPs. The observation that the $CD9^{hi}endoglin^{lo}$ fraction similarly is expanded selectively during recovery from APS-induced thrombocytopenia, a process dependent on intact TPO signaling, suggests that these cells make an important contribution to TPO-driven megakaryocyte and platelet production, not only in steady-state hematopoiesis but in also in times of acute need.

Materials and Methods

Mice. C57BL/6 mice were analyzed at age 7–10 wk. Mice expressing the *Aequorea victoria* GFP protein under the human ubiquitin C promoter were obtained from Jackson Laboratories (12). *PU.1*^{gfp} reporter strain (7) and mice carrying the *TPO*^{Tg} (13) and *Mpl*$^{-/-}$ (14) alleles were derived as previously described. Details of transplantation are given in *SI Materials and Methods*. Experimental thrombocytopenia was generated via tail vein injection of rabbit anti-mouse platelet serum (APS; Cedarlane). Experiments were performed using procedures approved by The Walter and Eliza Hall Institute of Medical Research Animal Ethics Committee.

Hematology and Histology. Blood was collected into tubes containing EDTA (Sarstedt), and platelet counts were obtained with an Advia 120 analyzer (Bayer). Analysis of erythrocytes and platelets was performed after blood was suspended in buffered saline glucose citrate buffer, and single-cell suspensions from bone marrow were prepared in balanced salt solution (*SI Materials and Methods*). Clonal analysis of bone marrow cells in semisolid agar cultures and liquid cultures of progenitor cells is described in *SI Materials and Methods*. Flow cytometry analysis was performed using an LSRII flow cytometer (Becton Dickinson), or cells were sorted using a FACSAria II (Becton Dickinson) flow cytometer after antibody staining with or without lineage depletion (*SI Materials and Methods*). Cytocentrifuge preparations were stained with May–Grunwald–Giemsa stain before microscopic examination. Images were acquired using a Nikon Eclipse E600 microscope, 4×/1.3 NA or 100×/1.3 NA oil objective with AxioCam Hrc and AxioVision 3.1 image acquisition software. Femurs were fixed in 10% vol/vol buffered formalin and embedded in paraffin, and 1- to 3-μm sections were stained with H&E for megakaryocyte enumeration via light microscopy.

ACKNOWLEDGMENTS. We thank Stephen Nutt and Sebastian Carotta for their generous gift of *PU.1*^{gfp} mice; Lauren Wilkins, Merle Dayton, Kelly Trueman, and Jaclyn Gilbert for excellent animal husbandry; and Jason Corbin and Janelle Lochland for excellent technical assistance. This work was supported by Australian National Health and Medical Research Council Program Grant 461219, by Independent Research Institutes Infrastructure Support Scheme Grant 361646, and by fellowships from the Australian National Health and Medical Research Council (to W.S.A. and A.P.N.); the Carden Fellowship Fund of the Cancer Council, Victoria (to D.M.); a Haematology Society of Australia New Zealand/AMGEN New Investigator Scholarship (to A.P.N.); a Cure Cancer Australia/Leukaemia Foundation postdoctoral fellowship (to A.P.N.); the Australian Cancer Research Fund; and a grant from the Victorian State Government Operational Infrastructure Support.

1. Metcalf D (2010) The colony-stimulating factors and cancer. *Nat Rev Cancer* 10: 425–434.
2. Bradley TR, Metcalf D (1966) The growth of mouse bone marrow cells in vitro. *Aust J Exp Biol Med Sci* 44:287–299.
3. Spangrude GJ, Heimfeld S, Weissman IL (1988) Purification and characterization of mouse hematopoietic stem cells. *Science* 241:58–62.
4. Okada S, et al. (1992) In vivo and in vitro stem cell function of c-kit- and Sca-1-positive murine hematopoietic cells. *Blood* 80:3044–3050.
5. Metcalf D, et al. (2009) Murine hematopoietic blast colony-forming cells and their progeny have distinctive membrane marker profiles. *Proc Natl Acad Sci USA* 106: 19102–19107.
6. Akashi K, Traver D, Miyamoto T, Weissman IL (2000) A clonogenic common myeloid progenitor that gives rise to all myeloid lineages. *Nature* 404:193–197.
7. Nutt SL, Metcalf D, D'Amico A, Polli M, Wu L (2005) Dynamic regulation of PU.1 expression in multipotent hematopoietic progenitors. *J Exp Med* 201:221–231.
8. Rieger MA, Smejkal BM, Schroeder T (2009) Improved prospective identification of megakaryocyte-erythrocyte progenitor cells. *Br J Haematol* 144:448–451.
9. Pronk CJ, et al. (2007) Elucidation of the phenotypic, functional, and molecular topography of a myeloerythroid progenitor cell hierarchy. *Cell Stem Cell* 1:428–442.
10. Nakorn TN, Miyamoto T, Weissman IL (2003) Characterization of mouse clonogenic megakaryocyte progenitors. *Proc Natl Acad Sci USA* 100:205–210.
11. Tronik-Le Roux D, Roullot V, Schweitzer A, Berthier R, Marguerie G (1995) Suppression of erythro-megakaryocytopoiesis and the induction of reversible thrombocytopenia in mice transgenic for the thymidine kinase gene targeted by the platelet glycoprotein alpha IIb promoter. *J Exp Med* 181:2141–2151.
12. Schaefer BC, Schaefer ML, Kappler JW, Marrack P, Kedl RM (2001) Observation of antigen-dependent CD8+ T-cell/ dendritic cell interactions in vivo. *Cell Immunol* 214: 110–122.
13. de Graaf CA, et al. (2010) Regulation of hematopoietic stem cells by their mature progeny. *Proc Natl Acad Sci USA* 107:21689–21694.
14. Alexander WS, Roberts AW, Nicola NA, Li R, Metcalf D (1996) Deficiencies in progenitor cells of multiple hematopoietic lineages and defective megakaryocytopoiesis in mice lacking the thrombopoietic receptor c-Mpl. *Blood* 87:2162–2170.